High concentration photovoltaic system with parallel kinematic solar tracker

International Journal of Applied Engineering Research ISSN 0973-4562 Volume 11, Number 19 (2016) pp. 9715-9722

High Concentration Photovoltaic System with Parallel Kinematic Solar Tracker

Stefano Mauro and Gabriele Biondi

Politecnico di Torino, Department of Mechanical and Aerospace Engineering
Corso Duca degli Abruzzi 24, 10129 Torino, Italy.

Abstract
The paper introduces a high concentration photovoltaic system developed at Politecnico di Torino. The system includes a new kind of solar tracker, based on a parallel kinematic mechanism, some high concentration photovoltaic modules and a heat recovery circuit intended for recovering heat from the chilling plant.
The paper in its first part describes in deep the design of the tracker and the control strategy used to drive it. In the second part the construction of a 2,8 kWp prototype is described and some results about experimental tests are shown.

Keywords: High concentration photovoltaic, parallel kinematic machine, heat recovery, solar tracker

INTRODUCTION

In the last years the use of renewable sources to produce electric power is greatly increased in order to comply with the need of reducing the emissions of greenhouse gases. In many countries photovoltaic plants have a large diffusion for the construction of domestic power plants, mainly placed on the roofs of the buildings.

At the same time large photovoltaic power plants are built in those countries where yearly solar irradiation is high and makes economically interesting the exploitation of this source.

When large photovoltaic (PV) power plant are built three different technologies should be considered in order to obtain the best economic return of the investment and the best exploitation of the soil: fixed photovoltaic modules, traditional PV modules on sun trackers or high concentration PV modules (HCPV), that must necessarily be assembled on high precision sun trackers.

It is well known since a long time that concentration technology strongly reduces the influence of the cost of solar cells on the total cost of the plant and of energy [1,2], and this makes economically possible the use of high efficiency triple junctions cells [3]. In this technology solar radiation is focused on a small solar cell by optical devices, which can be lenses or mirrors. The efficiency of cells increases with radiation, so the concentration ratio is a key factor to increase the total conversion efficiency of the plant and its productivity [4].

High concentration photovoltaic systems provide power output only if the solar radiation is correctly focused on the PV cell: this means that the misalignment error between the modules plane and the sun direction must be kept below a tolerance limit called “acceptance angle”. Whenever the misalignment should exceed this value the power output will drop to zero.

Because of this technologic constraint Sun trackers used to increase the production of traditional flat modules generally cannot be used for HCPV, they must be modified in their mechanical layout [5] and/or in control algorithms [6]. Fuzzy logic can be considered to increase control precision of mechanisms [7,8].

In order to build precise and stiff mechanisms, parallel architecture, which is widely applied in robotics [9-13] is a suitable solution. Within this work it is described a complete HCPV system with 2.8 kWp nominal power output in which the PV modules are oriented by a new parallel kinematic sun tracker. This has been developed by the authors upon a kinematic schematics proposed by Dunlop and Jones [14-17]. The system includes also a thermal circuit to recover heat from the cells to warm water for further application.

The paper describes the tracker, the technical solution applied for the construction of the prototype and of the HCPV modules, the layout of the experimental setup and the results of some functional tests.

TRACKER DESCRIPTION

The kinematic schematics of the tracker is shown in figure 1.

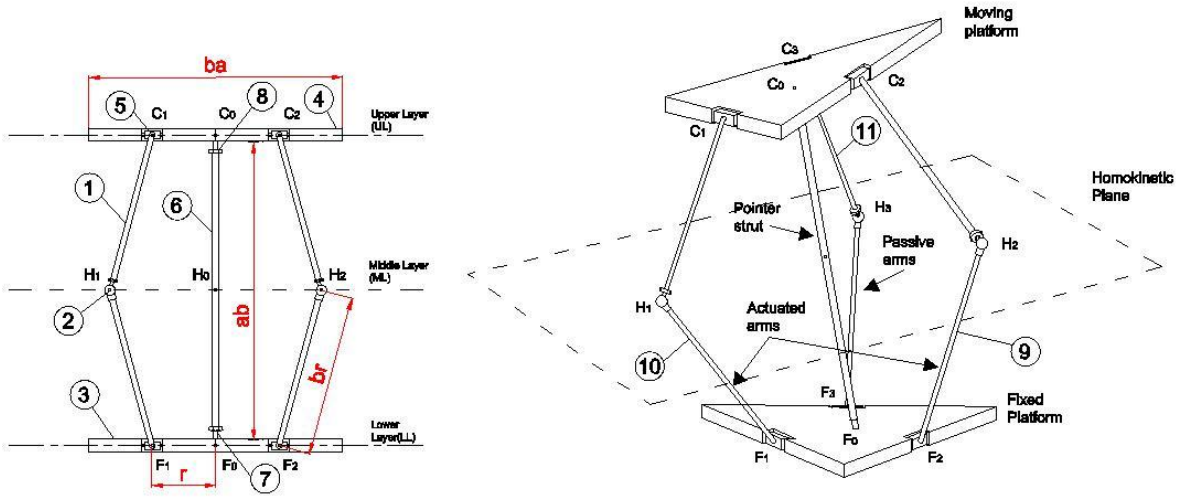

Figure 1. Kinematic schematics of the tracker

It is composed by six bars (1) connected in couples by three spherical joints (2). Each limb, composed by two bars, connects a lower fixed platform (3) with an upper mobile platform (4). The limbs are connected to the platforms by six revolute joints (5). The revolute joints are placed at the midpoints of two equilateral triangles, a first one in the plane of the lower platform (F_1,F_2,F_3) and a second in the plane of the upper one (C_1,C_2,C_3). The sides of the upper and lower triangles are equals. Finally a fourth limb, called "pointer strut", connects the two platforms and is fixed to them by two universal joints (7 and 8) placed in the incenters of the platforms.

Considering the right image in figure 1, the tracker is driven by controlling the angles of the beams hinged in F_1 and F_2, so limbs (9) and (10) are active while limb (11) is passive.

KINEMATIC ANALYSIS

The complete kinematic analysis of the mechanism, including the identification of its singularities, is described in [17].
In order to design the mechanism and to perform its control it is necessary to compute its direct kinematic, that links the position of the actuated limbs, expressed by angles β_1 and β_2 in figure 2, with Azimuth (α) and Zenith (ζ) angles. At the same time it is necessary to define an algorithm to compute the reverse kinematic of the mechanism, which links Azimuth and Zenith angles with the corresponding angles β_1 and β_2 of the actuated limbs.

Direct kinematics

In order to define the direct kinematic algorithm points H_i with i=0:3 must be defined. Point H_0 is the midpoint of the pointer strut, while points H_j with j=1:3 are the centers of the spherical joints of the three symmetrical limbs (see figure 1). These points always lay on plane π, which is marked as "homokinetic plane" in figure 1. The pointer strut is always perpendicular to the homokinetic plane, and hence the set of equation (1) is obtained.

$$\begin{cases} |\overrightarrow{F_0H_0}| = {}^1\!/_2\,|\overrightarrow{F_0C_0}| \\ \overrightarrow{F_0H_0}^T \cdot \overrightarrow{H_0H_1} = 0 \\ \overrightarrow{F_0H_0}^T \cdot \overrightarrow{H_0H_2} = 0 \end{cases} \quad (1)$$

The position of the points H_1 and H_2 is immediately computed by the values of the controlled angles β_1 and β_2 (se fig. 2) of the actuated limbs. Solving equations (1) the position of H_0 can be found and the angle of the point strut with it.
The Zenith angle is twice the elevation angle of the pointing strut, while the Azimuth angle of the platform is equal to the azimuth angle of the pointing strut.

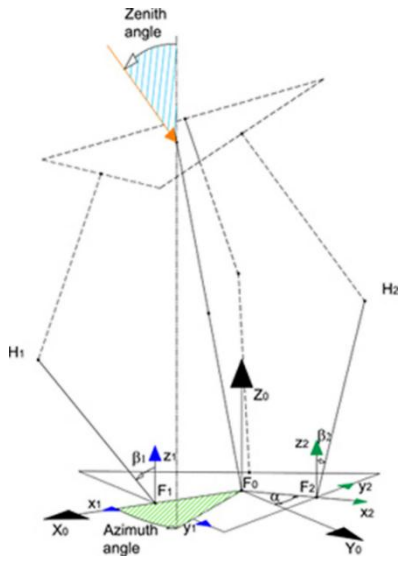

Figure 2. Reference systems, control angles, controlled angles

Introducing the reference system $X_0Y_0Z_0$ in figure (2), with origin in F_0 and X_0 pointing toward South, equations (1) can be solved and a system composed by a quadratic equation and two linear equations is found.

$$\begin{cases} \boldsymbol{rH_{0_z}^2 + wH_{0_z} + u = 0} \\ \boldsymbol{H_{0_x} = a_1 H_{0_z} + a_2} \\ \boldsymbol{H_{0_y} = a_3 H_{0_z} + a_4} \end{cases} \quad (2)$$

The coefficients in the set of equations 2 (r, w, u, a_1, a_2, a_3 and a_4) are not explicitly written for the sake of brevity but they can be calculated starting from the equation system 2 in a straightforward way. The complete description of the equations can be found in [15].

Solving equation (2) two solution are found: just one of them is acceptable in this context, and it is the one with an Azimuth angle ranging between 0° and 90°.

Reverse kinematic

A position of the π plane corresponds to each couple of Azimuth and Zenith angle. Each end of the actuated bar describes a circular trajectory around its hinge; the trajectory intersects the π plane in two points, each of which is a possible position of the spherical joint.

The circular trajectory of each actuated bar can be mathematically described as the intersection of a spherical surface centred in the centre of the revolute joint and of a plane perpendicular to the axis of the revolute joint and passing through the centre of the sphere.

The two possible positions of points H_1 and H_2 can be found solving two independent set of equations (3), with i =1,2,each of which describes the spherical surface, the plane perpendicular to the axis of the revolute joint and the π plane.

$$\begin{cases} \boldsymbol{(x - F_{ix})^2 + (y - F_{iy})^2 + (z - F_{iz})^2 = \overline{br}^2} \\ \boldsymbol{k_{ix}(x - F_{ix}) + k_{ix}(y - F_{iy}) + k_{ix}(z - F_{iz}) = 0} \\ \boldsymbol{\pi_x(x - H_{ix}) + \pi_x(y - H_{iy}) + \pi_x(z - H_{iz}) = 0} \end{cases} \quad (i = 1, 2) \quad (3)$$

The solution of the system is not reported in this paper and it can be found in [15].

DESIGN AND CONSTRUCTION

In order to design the tracker it is necessary to find a geometrical configuration that ensures the possibility of exploiting the solar radiation at any latitude and at any hour of the day. This involves that the workspace must span along the Azimuthal and Zenithal axis in the range [-180° ;- 180°] and [0 ; 90°], respectively. Three geometrical parameters contribute to the definition of the workspace: the length of the pointer strut, the length of each bar and the side of the triangles that identify the position of the hinges on the platforms. These parameters are indicated with $\overline{ab}$, $\overline{br}$,and $\overline{ba}$ respectively in figure 1.

The possible configuration can be analysed considering the $\frac{\overline{ab}}{\overline{br}}$ and $\frac{\overline{ba}}{\overline{br}}$ ratios. Each of them can vary in a range between 0.5 and 2, while lower or larger values will unbalance the machine.

All the possible combination of these ratios were considered, by spanning them with a step of 0.25, making a total of 49 possible configurations. For each of them the direct kinematic algorithm was run letting angles β_1 and β_2 span in the 30°- 125° interval by steps of 1°. In each case a plot in the Azimuth – Zenith plane was obtained in which a point was marked for each couple of values of β_1 and β_2, meaning that the point can be reached by the mechanism. The best configuration is the one that better fills the Azimuth-Zenith plane. After a second iteration with smaller ratios step it was found that the best configuration is the one with $\frac{\overline{ab}}{\overline{br}} = 0.8$ and $\frac{\overline{ba}}{\overline{br}} = 0.6$, with which 91% of the Azimuth-Zenith plane is reached. Figure 3 shows the actual workspace of the mechanism.

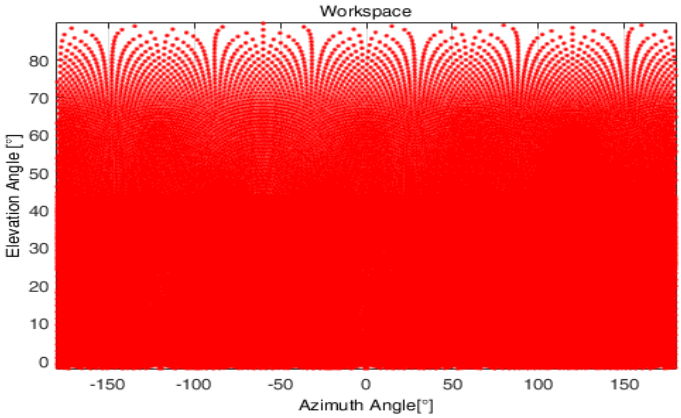

Figure 3. Filling of the Azimuth-Zenith plane

Figure 4 shows the singularities in the mechanism (in green) and the points that cannot be reached (in blue). The kinematic analysis to identify the singularities is described in [17]. Figures 3 and 4 show that the mechanism with the selected configuration fits the requirements for Sun tracking.

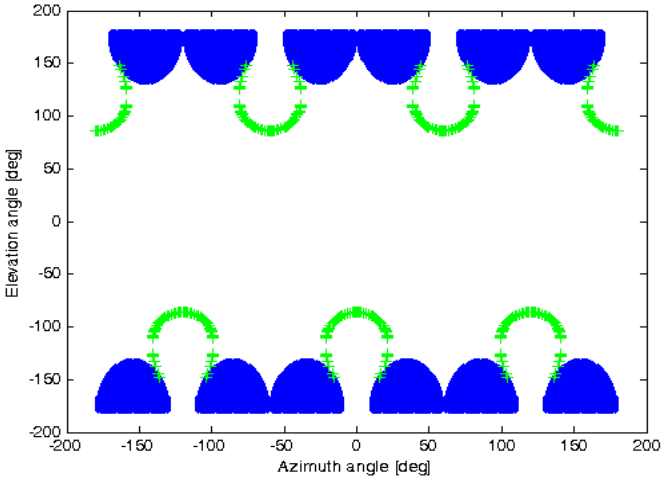

Figure 4. Singularities in the workspace

In order to move modules with a surface of 15 m^2, corresponding to a peak power of about 3 kWp with a module efficiency of 20%, the machine was designed considering a length $\overline{ba} = 1500\ mm$. The final design is shown in figure 5.

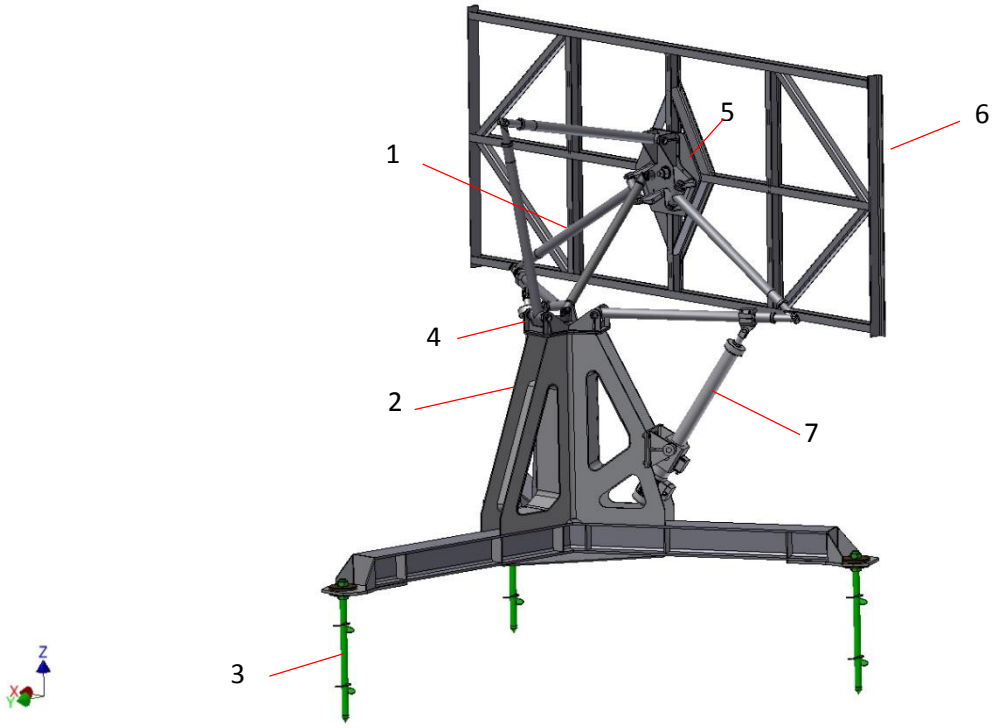

Figure 5. Final design of the tracker

The moving mechanism (1) is posed on a metal chassis (2) which is fixed to the soil by three screw systems (3). The lower platform (4) of the moving mechanism is on the top of the chassis, and the upper platform (5) holds a mobile frame (6) which provides a support for the PV modules. Actuation is provided by two actuators coupled each with a screw jack (7) fixed to the chassis.
In order to select the kind of actuation a trade off was carried out between electric, hydraulic and pneumatic power. Due to consideration about easiness of control, cost and sensitivity to control parameter and environmental condition [18-24], the decision was to use electric stepper motors.

HIGH CONCENTRATION PV MODULES

The high concentration PV modules were developed on the basis of high efficiency triple junction cells; solar radiation is concentrated by Fresnel lenses with a concentration ratio of 1020. Each module includes 15 PV cells and the same number of concentrating lenses (figure 6). Each cell is cooled by a liquid cooler (figure7) in order to exchange heat with a thermovector fluid which is used to warm water for thermal energy recovery. The acceptance angle is 0.3°.

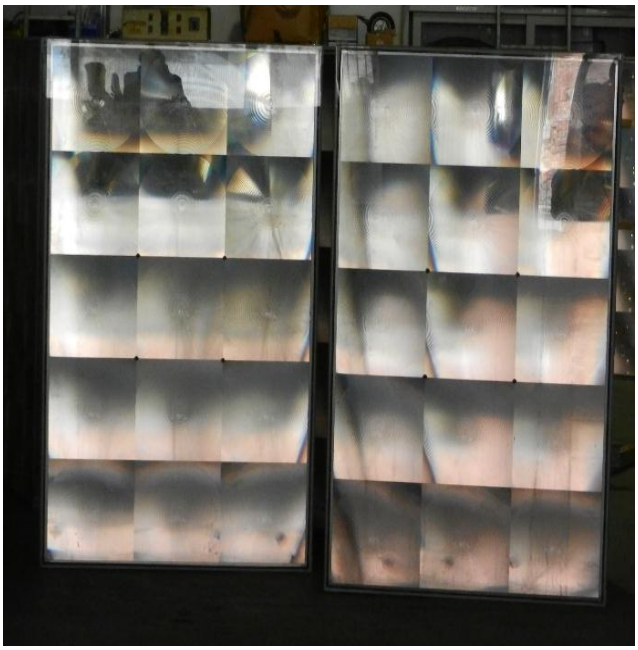

Figure 6. HCPV modules, front view

Figure 7. Heat exchangers

The nominal peak power of each module is 350 Wp at 800 W/m^2.

MACHINE CONTROL

The machine control was implemented on a Freescale microprocessor and developed in the Matlab environment. The system is a state machine in which three main blocks appear (figure 8):

- The starting position function, which drives the tracker to orientate the modules towards the expected position of the sun according to time, date and geographical location of the machine.
- The safety configuration, active in the case of high wind, which drives the modules to be oriented towards the zenith to reduce to a minimum the aerodynamic forces
- The active tracking function, in which the FV modules are precisely oriented towards the Sun in closed loop control with an orientation sensor

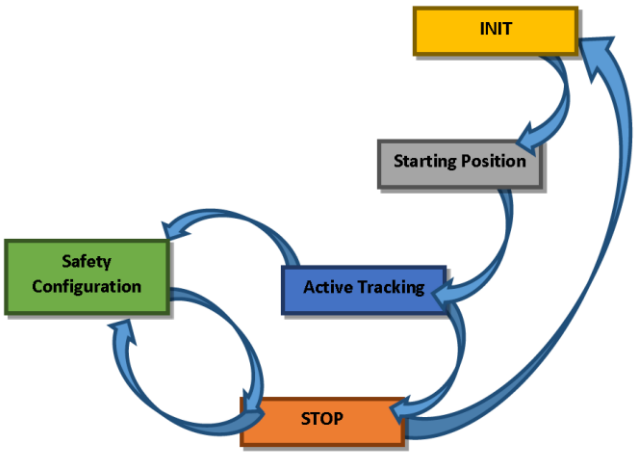

Figure 8. Organisation of the state machine

The state machine includes the Init and Stop functions: in the first one the machine turns on, check its systems and activates the starting position function; in the second one the machine stops in the event of absence of Sun or for an emergency and the control is given back to the Init function.
The control algorithm for the active tracking function is shown in figure 9. The control loop is closed by an orientation sensor composed by four sectors sensitive to solar radiation, divided by masking walls. The sensor provides four analogue signals which are proportional to the light radiations. They all are compared to a threshold in order to provide a True signal when the signal is larger than the threshold or a False signal in the opposite case.

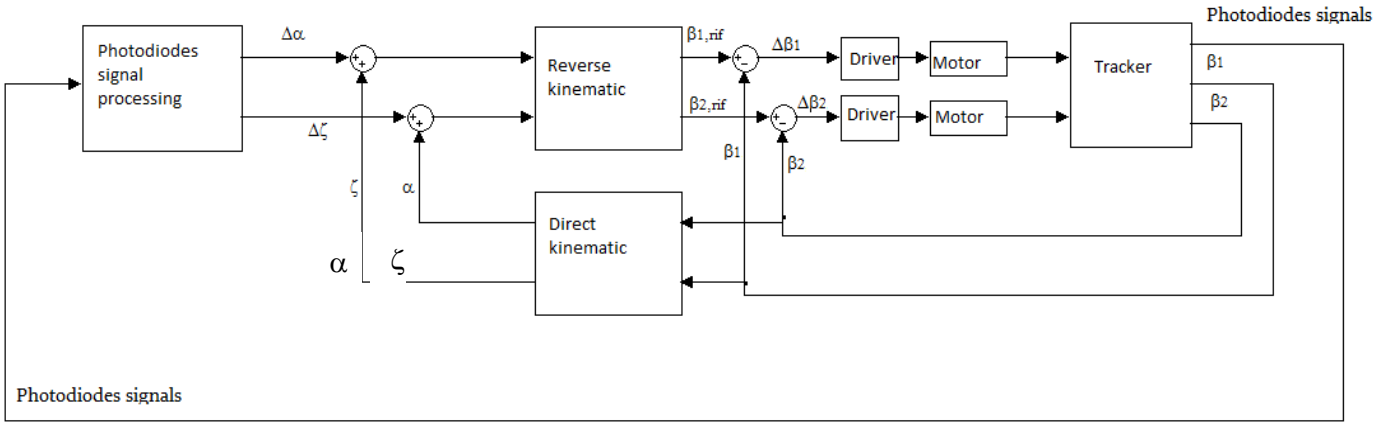

Figure 9. Block diagram of the control algorithm

The signal from the orientation sensor is decoded by the decoding map of table 1.

Table 1. Sensor decoding table

Case\sensor	1	2	3	4	Δζ	Δα
0	F	F	F	F	0	0
1	F	F	F	T	1	-1
2	F	F	T	F	1	1
3	F	F	T	T	1	0
4	F	T	F	F	-1	1
5	F	T	F	T	ERR	ERR
6	F	T	T	F	0	1
7	F	T	T	T	ERR	ERR
8	T	F	F	F	-1	-1
9	T	F	F	T	0	-1
10	T	F	T	F	ERR	ERR
11	T	F	T	T	ERR	ERR
12	T	T	F	F	-1	0
13	T	T	F	T	ERR	ERR
14	T	T	T	F	ERR	ERR
15	T	T	T	T	0	0

The map defines the direction along which the tracker must move in order to complete its alignment towards the Sun. When a misalignment exists at least one sensor is not fully enlightened. According to which sensors are not enlightened the table defines the direction in the azimuth-zenith space along which the tracker must move. According to the sensitivity of the sensors and to the acceptance angle of the PV modules the system performs step rotations of 0.2° in the selected direction. In the table positive steps are marked with 1 and negative ones with -1. So, for instance, in case 3 the tracker must increase the Zenith angle of 0.2° without changing the Azimuth value.
The step variation are added to the actual Azimuth and Zenith value in order to compute the new position reference, and the reverse kinematic algorithm computes the new references for the actuated angles □1 and □2. It must be pointed out that for each azimuth and zenith couple two couples of possible values for the actuated angles are calculated: it is then necessary to choose the closest to the actual ones. The actual values of the controlled angle are subtracted by the reference ones in order to compute the command for the step motors. Two high precision absolute encoders measures the actual position of the motor shafts to provide signals to measure the actual controlled angles β_1 and β_2 , which are processed by the direct kinematic algorithm to compute the Azimuth and Zenith angles. Signals from the encoders are also use to close the control loop of the servoaxis.

EXPERIMENTAL SET-UP

A full scale system was installed near to Turin, Italy, at coordinates 45°12'11.4"N, 7°53'06.4"E. Eight PV modules were assembled on the tracker for a total peak power of 2,8 kWp at 800 W/m^2 and a total surface of 13,6 m^2. The modules are connected to a standard 5 kWp standalone solar inverter coupled with a suitable set of batteries, as the miss of certification for the modules excluded grid connection. The heat recovery circuit includes a circulation pump, a 1000 litres tank and suitable circuitry to ensure stability and safety. Components were chosen from a standard solar heating equipment catalogue. A chiller was introduced in the circuit in order to simulate a thermal load.

Figure 10 shows the experimental set up.

Figure 10. Full scale experimental set up

TEST RESULTS

In March 2016 the system produced 14,7 kWh in a full day test in a clear sky day, during which the total radiation measured on the mobile surface was 6,7 kWh/m^2 for a total irradiance of 91,4 kWh. At the same time the thermal power produced was 220,8 MJ. Long term tests are still running.

The total energy production shows that the system was continuously producing power, that confirms the capability of keeping the alignment error always below the acceptance angle. This means that the mechanical design and the control algorithm satisfy the requirements for HCPV.

CONCLUSIONS

The system developed in this work showed to be capable to ensure continuous production with a high concentration photovoltaic system by using a solar tracker with a completely new design, based on a parallel kinematic mechanism.

The system recovers heats from the chilling fluid and provides power to warm water for further applications. The system can be employed as energy unit to supply single family houses.

ACKNOWLEDGMENTS

The authors wish to thank Regione Piemonte and its Poligh innovation center for its financial support within the "Solarbuild" project – POR FESR 2007 – 2013

REFERENCES

[1] Peharz, G., Dimroth, F., 2005, "Energy payback time of the high-concentration PV systems FLATCON®", Progress in photovoltaics: Research and applications, vol. 13, pp. 627-634. DOI: 10.1002/pip.621

[2] Cotal,H., Fetzer,C,, Boisvert, J., Kinsey, G. King, R ,Hebert, P., Yoon, H. and Karam, N., 2009, "III-V multijunction solar cells for concentrating photovoltaics, Energy and Environmental Science, vol. 2, pp. 174-192. DOI: 10.1039/b809257e

[3] King, R. R., Bhusari, D., Larrabee, D., Liu, X.-Q., Rehder, E., Edmondson, K., Cotal, H., Jones, R. K., Ermer, J. H., Fetzer, C. M., Law, D. C. and Karam, N. H. (2012), Solar cell generations over 40% efficiency. Prog. Photovolt: Res. Appl., 20: 801–815. doi:10.1002/pip.

[4] Nishioka, K., Takamoto, T., Agui, T., Kaneiwa, M., Uraoka, Y. and Fuyuki, T.., 2006, "Annual output estimation of concentrator photovoltaic systems using

high-efficiency InGaP/InGaAs/Ge triple-junction solar cells based on experimental solar cell's characteristics and field-test meteorological data", Solar Energy Materials & Solar Cells, vol. 90, pp. 57-67. DOI: 10.1016/j.solmat.2005.01.011

[5] Yazidi, A., Betin, F., Notton, G., Capolino, G.A., 2006, "Low cost two-axis solar tracker with high precision positioning", *Proceedings of the 1st ISEIMA International Symposium on Environment identities Mediterranean area*, Corte-Ajaccio, pp. 211-216. DOI: 10.1109/ISEIMA.2006.344932

[6] Rubio, F.R., Aracil, J., 1997, "Design of a Combined Tracking Control System", Control Engineering Practice, vol. 5, pp. 23-31. DOI: 10.1016/S0967-0661(96)00203-1

[7] Chojnacki, J.A., 2005, "Application of Fuzzy Logic Neural Network Controllers in PV Systems", *Proceedings of the 20th European Photovoltaic Solar Energy Conference*, Barcelona, pp. 2269-2272

[8] Mattiazzo, G., Mauro, S., Raparelli, T., Velardocchia, M., 2002, "Control of a six-axis pneumatic robot", Journal of Robotic Systems, 19 (8), pp. 363-378,DOI: 10.1002/rob.10046

[9] Mauro S., Gastaldi L., Pastorelli S., Sorli, M., (2016), "Dynamic flight simulation with a 3 d.o.f. parallel platform" International Journal of Applied Engineering Research, 11(18), pp. 9443-9445.

[10] Portman, V.T., Sandler, B.-Z., Zahavi, E., 2001, "Rigid 6-dof parallel platform for precision 3-d micromanipulation", International Journal of Machine Tools Manufacture, vol. 41, pp. 1229-1250. DOI: 10.1016/S0890-6955(01)00027-X

[11] Tahmasebi, F., 2006, "Kinematics of a New High-Precision Three-Degree-of-Freedom Parallel Manipulator", ASME Journal of Mechanical Design, vol. 129 (3), pp. 320-325. DOI: 10.1115/1.2406103

[12] Li, Y., Xu, Q., 2008, "Stiffness analysis for a 3-PUU parallel kinematic machine", Mechanism and Machine Theory, vol. 43, pp. 186-200. DOI: 10.1016/j.mechmachtheory.2007.02.002

[13] Pastorelli, S., Battezzato, A., 2009, "Singularity analysis of a 3 degrees-of-freedom parallel manipulator" Proceedings of the 5th International Workshop on Computational Kinematics, 2009, 331-340

[14] Dunlop,G.R. and Jones, T.P., 1999, "Position analysis of a two DOF parallel mechanism – the Canterbury tracker", Mechanism and Machine Theory 34 (1999) 599-614

[15] Mauro, S., Scarzella, C., 2010, "Parallel mechanism for precision sun tracking", ASME 2010 10th Biennial Conference on Engineering Systems Design and Analysis, ESDA2010, 2, pp. 17-22. Instanbul, Turkey, July 12-14, 2010, DOI: 10.1115/ESDA2010-24100

[16] Battezzato, A., Mauro, S., Scarzella, C., 2012, "Developing a parallel kinematic solar tracker for HCPV", ASME 2012 11th Biennial Conference on Engineering Systems Design and Analysis, ESDA 2012, 2, Nantes, France, July 2-4, 2012, pp. 459-464. DOI: 10.1115/ESDA2012-82193

[17] Mauro, S., Battezzato, A., Biondi, G. and Scarzella, C., 2015, "Design and test of a parallel kinematic solar tracker", Advances in Mechanical Engineering, December 2015 7: doi:10.1177/1687814015618627

[18] Mattiazzo, G., Mauro, S., Guinzio, P.S., 2009, "A tensioner simulator for use in a pipelaying design tool", Mechatronics, 19 (8), pp. 1280-1285, doi: 10.1016/j.mechatronics.2009.08.004

[19] Mauro, S., Pastorelli, S., Mohtar, T., 2014, "Sensitivity analysis of the transmission chain of a horizontal machining tool axis to design and control parameters", Advances in Mechanical Engineering, 2014, doi: 10.1155/2014/169064

[20] Mauro, S., Pastorelli, S., Johnston, E., 2015, "Influence of controller parameters on the life of ball screw feed drives", Advances in Mechanical Engineering,7(8), pp.1-11. DOI:10.1177/1687814015599728

[21] Jacazio, G., Pastorelli, S., Sorli, M., 2008 "A prognostics model for detecting the irreversibility margin of non-reversible electromechanical actuators", Int. Conf. on Prognostics and Health Management, PHM 2008, Denver; United States art. N. 4711457

[22] Sorli M., Figliolini G., Pastorelli S., Rea P., 2005 "Experimental identification and validation of a pneumatic positioning servo-system". Power Transmission and Motion Control, PTMC 2005, pp. 365-378.

[23] Sorli M., Gastaldi L., 2009, "Thermic influence on the dynamics of pneumatic servosystems", Journal of Dynamic Systems, Measurement and Control 131(2): pp. 1-5.

[24] Balossini, G., Gastaldi, L., Jacazio, G., Magnani, A., 2013, "Hydraulic actuation system with active control for the lateral suspensions of high speed trains". International Journal of Heavy Vehicle Systems,;20 (3); pp. 236-252.

[25] Jacazio, G., Gastaldi, L. 2016 "Robust pressure control improves the performance of redundant fly-by-wire hydraulic actuators". International Journal of Applied Engineering Research, 11(15), pp. 8590-8597